In-situ photoelectrochemical measurement of phthalic acid on titania

Shanqing Zhang[a,*], William Wen[a], Hongzhong Zhang[a,b] , and Huijun Zhao[a]

[a]Australian Rivers Institute and Griffith School of Environment
Gold Coast Campus, Griffith University
QLD 4222, Australia

[b]Zhengzhou University of Light Industry, Henan Provincial Key Laboratory of Surface and Interface Science, Zhengzhou, Henan 450002, China

Corresponding Authors
Dr. Shanqing Zhang
Tel: (61-7) 5552 8155
Fax: (61-7) 5552 8067
Email: s.zhang@griffith.edu.au

Abstract

An *in-situ* photoelectrochemical method is proposed to determine adsorbed phthalic acid (PA) on the TiO_2 surface in a sensitive, reproducible and accurate manner. The pre-adsorbed PA in the dark and the diffused PA from organic solution can be mineralized simultaneously under UV illumination due to the strong UV-induced oxidation power of TiO_2. By controlling the UV illumination, the amount of adsorbed PA on TiO_2 surface was determined in the presence of PA in a small time scale (e.g., second), eliminating the washing step after the adsorption reaction. This provides a convenient and effective alternative to study adsorption behaviour on TiO_2. The proposed method was applied to determine the adsorption equilibrium constant of PA.

Key Words: *in-situ* measurement, adsorption, TiO_2, photoelectrochemistry.

1. Introduction

Adsorption characteristics of organic compounds at the TiO_2–liquid interface play an important part on the photocatalytic oxidation processes [1-8]. In order to improve the efficiencies of the photocatalytic oxidation processes, adsorption kinetics and thermodynamics at the interface should be investigated quantitatively. The measurement of adsorption amount at the TiO_2 surface is inevitably involved in the investigation of adsorption process. Traditionally, the amount of adsorbed species on the TiO_2 nanoparticles can be determined directly via the following steps [8-10] : 1) sufficient amount of TiO_2 nanoparticle slurries is added in adsorbate solution in order to ensure that measurable amount of adsorbates to be adsorbed from the solution by the adsorption process; 2) TiO_2 slurry is separated from the solution using filtration or centrifuge instrument; 3) post-adsorption washing with water to remove residue solution on the particles; 4) dissolve the adsorbates with organic solvent; 5) determination of the adsorbate amount using chemical analysis tools, e.g., UV-vis spectrophotometer or HPLC. This method is often insensitive, low precision, tedious and time-consuming. More importantly, this method cannot provide reliable measurement in a short time scale (e.g., seconds). This is mainly because adsorption time cannot be quantified accurately due to the fact that adsorption reaction continues during the separation of TiO_2 nanoparticles from the reaction solution.

Due to the aforementioned problems, many attempts have been attracted to directly probe and determine the adsorbate amount using various ways, such as sum frequency generation spectroscopy [11, 12], photoelectrochemical techniques [8], IR [13], Raman spectroscopy [14], UV absorption spectroscopy [15], electrophoresis [16], quartz crystal

microbalance (QCM) [17], and even combined techniques, such as, incorporation of photoelectrochemical and spectroscopic techniques, i.e., Attenuated Total Reflection Inferred (ATT-IR), and Resonance Raman Spectroscopy [18]. These attempts have provided significant insights into the adsorption process in time course (i.e., QCM method). However, difficulties remain for *in-situ* determination of the adsorption amount for small molecules in aqueous solution in a very short time scale.

In our previous work, an *ex-situ* photoelectrochemical method was developed to measure the amount of phthalic acid (PA) adsorption on TiO_2 electrode surface [8]. In the *ex-situ* method, adsorption of PA onto the TiO_2 surface was carried out by immersing a TiO_2 electrode into a PA solution for a given period of time, and then the electrode was washed by the supporting electrolyte and transferred to a photoelectrochemical reactor where the adsorption amount of PA was measured. In contrast, in this study, we propose and develop an *in-situ* photoelectrochemical method where both the adsorption process and the photoelectrochemical measurement are conducted in the same solution of the target organic compound in the same reactor. This arrangement of experiment has overcome the aforementioned short-time scale problems associated with the quantification of the adsorbate amount on the TiO_2 surface by eliminating the washing step. The adsorption process of PA on the TiO_2 was investigated to demonstrate the applicability of the proposed *in-situ* approach. PA is an aromatic compound with two carboxyl groups ($H_2C_8H_4O_4$, $pK_{a1} = 2.95$, $pK_{a2} = 5.41$)[19] which are known to strongly adsorb to the surface of TiO_2 [20]. The speciation of PA at different pH was discussed in our previous work. At pH 4, the dominant form of PA is $HC_8H_4O_4^-$ that can be most favourably adsorbed to TiO_2 surface [8]. The proposed *in-situ* method is expected to be a

simple and accurate alternative for determination of the adsorption amount for small molecules in a very short time scale.

2. Experimental

2.1 Materials. Indium Tin Oxide (ITO) conducting glass sheets (8-10Ω/square, Delta Technologies Limited) were used as substrates for TiO_2 film coating. All chemicals were of analytical grade and purchased from Sigma-Aldrich unless otherwise stated. All solutions were prepared using high purity deionised water (Millipore Corp., 18MΩcm). PA solution was prepared by dissolving potassium hydrogen phthalate (KHP) into 0.1M $NaNO_3$ solution and adjusting the solution pH to 4.0 with HNO_3.

2.2 Preparation of the nanoporous TiO_2 film electrode.

Aqueous TiO_2 colloid was prepared by hydrolysis of titanium butoxide according to the method described by Nazeeruddin [21]. The TiO_2 nanoparticles were immobilized on the ITO surface using dip coating technique. The coated electrodes were dried in air, and then calcined in a muffle furnace at 700ºC temperature for 16h in air. The thickness of TiO_2 porous films was ca. 500nm as measured with a surface profilometer (Alpha-step 200, Tencor Instrument). The details of fabrication procedures and characterization information were described in our previous works [22, 23].

All photoelectrochemical experiments were carried out in a three-electrode electrochemical cell with a quartz window for illumination [23], containing Ag/AgCl as a reference electrode, Pt net as a counter electrode and the resulting TiO_2 electrode as a working electrode. 0.1M $NaNO_3$ (pH 4.0) was chosen as the supporting electrolyte throughout all the experiments. The working electrode surface area exposed to solution

and UV light was a circle with a diameter of 10 mm. Illumination was achieved with a 150W xenon arc lamp light source (Trusttech, Beijing, China). To minimise the heating of the TiO_2 electrode from the infrared fraction of the xenon light, the xenon light beam was passed through an UV-band pass filter (UG-5, Schott) prior to illuminating on the electrode surface. Light intensity at the electrode surface was 6.6mW/cm^2 unless otherwise stated. An optical shutter with an aperture of 20mm (Copal Co, Japan) was used as optical switch to reproducibly control the ON and OFF of the UV illumination.

3. Results and Discussion

The TiO_2 thin-film electrode used in this study was a mixed-phase electrode, containing 96.8% of anatase and 3.2% of rutile. The structural characteristics of the electrode were reported in details in our recent work [23]. Under sufficient UV illumination, different organic compounds in a low concentration range, despite their difference in chemical entities, can be stoichiometrically mineralized at the mixed-phase TiO_2 electrode under diffusion-controlled conditions due to the synergetic effect of the rutile and anatase phase [23]. The general equation for mineralization can be summarised as follows:

$$C_yH_mO_jN_kX_q + (2y-j)H_2O \rightarrow yCO_2 + qX^- + kNH_3 + (4y-2j+m-3k)H^+ + (4y-2j+m-3k-q)e^- \quad (1)$$

where the elements present are represented by their atomic symbols and *X* represents a halogen element respectively. The stoichiometric ratio of elements in the organic compound is represented by the coefficients *y*, *m*, *j*, *k* and *q*. The number of electron transfer (n) in the complete oxidation process is equal to $4y-2j+m-3k-q$. Our previous adsorption study using *ex-situ* photoelectrocatalytic method had demonstrated that the oxidation of adsorbed species follows the same principle as described by Eqn. 1.

3.1 The photoelectrochemical property of the TiO_2 electrode

The electron transfer process of Eqn. 1 during the photoelectrocatalytic reaction was well established [3, 22]. Generally, organic compounds are more readily oxidised than water by the photoanode [24]. The oxidation of water and organic compounds takes place at the TiO_2 surface under the UV illumination, and the role of the applied potential bias was mainly used to collect electrons generated from the above processes [25]. The photoelectrochemical behaviour of the TiO_2 electrode was firstly investigated using linear sweeping voltammetry (LSV) in PA solution. The photocurrent-potential characteristics of the electrodes were obtained in the presence and absence of PA by LSV at a scanning rate of 10 mV/s between −0.40 and 0.60V vs Ag/AgCl. (Fig. 1). In the dark (with no UV illumination), no significant current was observed for the blank (i.e., 0.1 M $NaNO_3$) and PA solution. This suggests that no typical electrochemical oxidation of water and PA occurs between −0.40 and 0.60V in the above scenarios.

As shown in Fig. 1a, under UV illumination, the photocurrent increases dramatically with the potential bias in a low potential region (i.e., -0.4 to -0.1V) and then levels off with a very small slope in a high potential region (i.e., -0.1 to +0.6V). It was observed that the LSV curves at different concentration (from 2.5 to 125μM PA) share almost identical slope with the LSV curve of the blank in the high potential region. The LSV curve for the blank (with 0 μM PA) involves mainly the oxidation of water and some minor resistance effect between TiO_2 nanoparticles and ITO glass [26]. The LSV curves of different PA concentration in Fig. 1b were obtained by subtracting the corresponding LSV values of the blank, which removes the above effects of the blank. Therefore, the *i-E* curves of Fig. 1b can be considered as a result from the oxidation of different PA concentration. Typical

saturated photocurrents at different PA concentration could be observed when the sweeping potential was greater than 0.0V. This suggests that, for a given PA concentration, the photocurrents were independent to the potential in this potential range, which was similar to the photocurrent–potential relationship obtained from a pure anatase TiO_2 electrode in a PA solution as discussed in our previous work [8]. Such photocurrent–potential relationship may be explained as follows. For a given light intensity, the concentration of photo-generated electron–hole pairs (or the production rate of electron–hole pair) is constant. The magnitude of the photocurrent, i.e., the actual rate of electrons reaching the back contact, depends on two factors: the electron transport in the film and the photohole capture process at the TiO_2–solution interface. Before the photocurrent reaches saturation with respect to potential (i.e., from -0.4V to 0.0V), the electron transport across the film is the rate-determining step. As a result, a monotone increase LSV curve is obtained. When the rate of the electron transport is not increased by increasing the applied potential (i.e., from 0.0V to +0.5V), the rate of reduction of the photo-generated hole becomes the limiting factor resulting in photocurrent saturation. The saturation suggests that the electrons due to the photoelectrochemical oxidation of PA were collected and transferred to the counter electrodes completely which is evidenced in Fig. 1b. In this study, a +0.30V potential bias was selected for all subsequent experiments. This was chosen such that the potential bias was sufficient to suppress the recombination of photo-induced electron–hole pairs but not so positive to electrochemically oxidise water and PA at the ITO surface, which complicates the adsorption investigation.

3.2 In-situ transient photocurrent response

Under a constant applied potential bias, a photocurrent spike can be observed from a TiO_2 porous film electrode when the UV light is illuminated on the electrode surface. Fig. 2 shows the transient photocurrent responses obtained at +0.30V applied potential with different dark time duration in a 5 μM PA (pH 4.0) solution containing 0.10 M $NaNO_3$. A sharp photocurrent spike was observed immediately after the light was switched on, the photocurrent then decayed gradually to a steady photocurrent. This phenomenon has been reported in an investigation of photoelectrochemical oxidation of oxalate at TiO_2 porous film electrodes [3]. The peak current in Fig. 2 is considered as the photoelectrochemical consumption of adsorbed organic compound rather than a double layer charging and discharging process [3]. The magnitude and area of the photocurrent spike increased as the time of the dark period increased. Such a transient response of photocurrent has long been observed and studied [3, 8]. The transient response is mainly due to Faradic photoelectrochemical degradation of adsorbed PA [26]. This is because the time domain of the transient observed was much longer than the normal capacitance response of space charge layer and electric double layer, and the area under the current spike was found to be dependent on the non-illumination time length and the PA concentration, which are not the characteristics of charging and discharging current.

The steady-state photocurrent was independent of the time of dark period, which is another characteristic of the transient photocurrent profiles. According to the semi-empirical treatment of steady state mass transfer method [27], under the diffusion control condition, the limiting photocurrent (i_L) can be given by:

$$i_L = \frac{nFADC}{\delta} \qquad (2)$$

where, n is the number of electrons transferred in the complete mineralization of organic compounds (see Eqn.1), F is the Faraday constant, A is the apparent surface area of the electrode, D and δ refer to the diffusion coefficient of the organic compound and the thickness of the effective diffusion layer respectively, and C is the bulk concentration of the organic compound.

Fig. 3a depicts typical photocurrent responses of TiO_2 thin-film electrode in blank and PA solutions under UV illumination. The steady state photocurrent (i_{ss}) is the aggregate current resulted from the oxidation of water (steady state photocurrent i_{blank}) and oxidation of PA limited by a diffusion control process (steady state current i_L).

In practise, the i_L is the difference of i_{ss} and i_{blank}, i.e.:

$$i_L = i_{ss} - i_{blank} \qquad (3)$$

Fig. 3b shows the plot of PA concentration against the net photocurrents (i_L) that were calculated using Eqn. 3. The excellent linearity between i_L and the PA concentration was observed at low PA concentrations (<300 μM PA), which suggests that, within the low PA concentration range, the mass transport of PA from the bulk solution to the electrode surface was the rate-limiting step among the interfacial processes, which supports Eqn. 2. This phenomenon was observed for other organic compounds as well [23]. Our previous work demonstrated that under the diffusion control conditions, all the organic molecules diffused to the electrode surface could completely be mineralized [23].

Theoretically, photo holes cause three competitive processes at the TiO_2 surface: the oxidation of water, the oxidation of PA, and electron-hole surface recombination. Though PA is more preferentially oxidised than water, the competition for photo holes between

PA and water is significant at high PA concentrations. In the case of low PA concentrations (i.e., in the range of μMs), the competition for photo holes between low concentration of PA (i.e., μM of PA) and extremely high concentration of water molecules (i.e., 56M water) can be neglected. Therefore, the current result from the oxidation of water can be considered to be relatively constant and the increase of i_L is more likely due to the decrease of surface carrier recombination that in turn was beneficial from the availability of PA. This analysis is evidenced by the fact that i_L is directly proportional to the PA concentrations at low concentration range while it is leveled off at higher concentrations (see Fig. 3b).

The effect of light intensity on the photo currents under a constant potential was investigated. It is observed that the increase of the light intensity will increase the total current (i_{ss}) and i_{blank}, which is obviously due to the increase of photo holes resulting from the injection of more photons. i_L at different light intensity are subsequently plotted against PA concentration in Fig. 3b. Interestingly, the increase of the light intensity does not increase the sensitivity to PA (i.e., the slope in Fig. 3b), but it extends the linear range of the calibration curve. This is because this increase in i_{ss} was mainly contributed by the increase of the blank photocurrent (i_{blank}) generated from water oxidation. The excess of photo holes are consumed by water due to the concentration of water (56M) is dramatically higher than the organic compound concentration. The fact that the i_L is independent of the illumination intensity at low PA concentrations (< 100μM PA under all indicated light intensity) again suggests that the competition for photo holes between water and PA is negligible. More importantly, this confirms that the i_L is under the diffusion control of PA.

3.3 The principle of in-situ adsorption measurement

The diffusion-controlled photocurrent in Fig. 3b also implies that, at the time when steady-state current is attained, the PA concentration and water concentration at the TiO_2 electrode surface can be assumed to be zero. In other words, a perfectly clean surface (i.e., un-adsorbed surface) of TiO_2 can be obtained at the steady state. This is of importance as this characteristic is an excellent indication of the completion of consumption of adsorbates, i.e., pre-adsorbed organic compounds and water during the dark time. Also, a completely clean surface is an ideal starting point for adsorption reaction study. This allows the *in-situ* measurement of adsorption amount and forms the theoretical base for the proposed *in-situ* method. The attainment of the diffusion-controlled photocurrent is essential for the proposed adsorption measurement method.

The solid line in Fig. 4 is a typical photocurrent profile upon the UV illumination and the dash line is an integration reference line. As aforementioned, the steady-state photocurrent is the overall current originated from the photoelectrocatalytic oxidation of organic compounds and water molecules. The photoelectrocatalytic oxidation of organic compounds was under the diffusion control of the organic species, e.g., PA., while the oxidation rate of water is constant due to the invariable water concentration (i.e., 56M). In contrast, the photocurrent of the spike consists of the oxidation current of the adsorbates (including adsorbed organic compounds and adsorbed water molecules) and the steady-state current. The attainment of steady-state current indicates the mass transport at the electrode surface is under the control of the diffusion, and suggests that the adsorbates on TiO_2 surface have been mineralized completely. Based on the above observation and hypothesis, we can conclude that the net photocurrent (i_{net}) of the spike

photocurrent (i) and the steady state current (i_{ss}) is the photocurrent originated from oxidation of adsorbates. i.e., $i_{net} = i - i_{SS}$. By integrating this net current using the integration reference line in Fig. 4 and Eqn. 4, we obtain the charge (Q_{net}), i.e., the shaded area shown in Fig. 4.

$$Q_{net} = \int i_L dt = \int (i - i_{SS}) dt \qquad (4)$$

Though it is possible that the water can be adsorbed in the presence of organic compounds, the contribution from the water adsorption can be neglected because the adsorption kinetics of water is slow. More importantly, organic adsorbates can compete adsorption sites with adsorbed water molecules. Nevertheless, the adsorption of strong adsorbates, such as PA, is the dominant process in aqueous solution.

For a specific organic compound, the number of electron transfer (n) during the mineralization process can be calculated according to Eqn. 1, e.g., n = 30 for PA [25]. Once the number of electrons (i.e., Q_{net}) oxidized at the TiO_2 surface is determined, according to Faraday's Law, we can quantify the amount of adsorbed molecule using Eqn. 5. Therefore Q_{net} can be considered as a measure of the amount of adsorbates on TiO_2 surface.

$$moles = Q_{net} / (nF) \qquad (5)$$

3.4 Effect of PA concentration

The relationships between the net charge (Q_{net}) and the *in-situ* pre-adsorption time at different PA concentrations in a long time scale (i.e., 30min) and a short time scale (i.e., 30s) were obtained using Eqn. 4 as shown in Fig. 5a and 5b, respectively. Fig. 5 indicates that Q_{net} increased dramatically for the first 30s, and then increased slowly and

subsequently levelled off, which suggests that adsorption equilibrium was attained. Fig. 5a shows that the Q_{net} increased with the increase of adsorbate concentration and time, and that it took less time for high adsorbate concentration to reach adsorption equilibrium state. For example, the adsorption equilibrium could be attained in <20 min at a relatively high concentration of PA (i.e., 25 μM). In contrast, at a low adsorbate concentration (e.g., 2.5 μM), the net charge increased much slower with pre-adsorption time than that at a high adsorbate concentration. This was similar to the observation at the anatase phase TiO_2 electrode using *ex-situ* method [8].

With conventional chemical analytical technique, it is very difficult to investigate the fast adsorption process (e.g., the first 30s) in an accurate and reproducible manner. This is mainly due to the lack of effective method to accurately quantify the adsorption reaction time. In this experiment, the accurate control of UV-light shut-off time provides a definite reference point to quantify the adsorption reaction time and a perfect zero adsorption point to quantify the adsorption amount. Fig. 5b shows the adsorption behaviour in the short time scale, which was obtained by using the proposed *in-situ* method. As shown in Fig. 5b, Q_{net} increased linearly with adsorption time for a given PA concentration in the first 30s. This demonstrates that the PA diffusion prevails over other steps of the adsorption process during the first 30s, which verifies our previous hypothesis.

For further quantitative analysis, linear regression was conducted for the Q_{net} at different PA concentrations with the adsorption in Fig. 5b, respectively. The slopes and intercepts on the *y* axis of the trendline equations for the different PA concentrations were obtained

and listed in Table 1. Table 1 indicates that the slope increased with the PA concentration increase while the intercept values are all positive and relatively constant.

The slopes in Table 1 represent the adsorption rates at different PA concentrations. In order to quantitatively investigate the relationship between adsorption rate and PA concentration, the slope values were plotted against PA concentration (see Fig. 6). Excellent linearity ($R^2 = 0.9988$) could be observed between the adsorption reaction rates and PA concentrations. This linear relationship between the adsorption rate and PA concentration here is a direct reflection of Fick's law of diffusion (Eqn. 2). As aforementioned, when a steady-state current is reached, the mass transport of PA from bulk solution to the TiO_2 electrode surface is limited by the PA concentration. In other words, at this time, the PA concentration at the TiO_2 electrode surface can be considered as zero. When UV light is switched off, the photoelectrocatalytic degradation reaction (Eqn. 1) stops, and the net adsorption reaction of PA starts on the TiO_2 surface. Interestingly, slopes of PA diffusion-limiting oxidation current, as indicated in Fig. 3b, is almost identical to the PA diffusion-limiting adsorption rate (see Fig. 6), sharing with the same value and unit (i.e., $\mu A/\mu M = \mu C \cdot s^{-1}/\mu M$). This is because both the adsorption in the dark and the photoelectrocatalytic oxidation processes under UV illumination were controlled by the diffusion of PA. This can be considered as a significant evidence supporting our hypothesis. This can be explained by the Fick's law, i.e., the adsorption amount was proportional to a given adsorption time when the adsorption reaction rate is limited by the mass transport of the adsorbate (See Fig. 5b). It is to note that this is only valid in low adsorbate concentration range and at the time of low surface coverage of the adsorption surface (i.e., sufficient adsorption reaction sites). The former condition assures

that the mass transport is sufficiently slow because of the small concentration gradient, while the latter one guarantees an adequately fast adsorption reaction rate. The common slopes of Fig. 3b and Fig. 6 also suggest that the PA diffusion limiting net current can be used to estimate the maximum adsorption amount, which is simple and straightforward. This is because the adsorption process can never exceed the mass transport of adsorbate. In a longer time domain, the adsorption rate decreased with the increase of the surface coverage of the interface (see Fig. 5a). In this case, the adsorption rate will be limited by the availability of unadsorbed sites rather than the mass transport of the adsorbates.

The positive small intercepts shown in Table 1 is very likely due to the water adsorption in dark time. This is because the water concentration (i.e., 56M) was predominantly higher than the PA concentrations and inevitably contributed a small amount of charge to Q_{net}, despite of the weak water adsorption nature of TiO_2 surface in the presence of strong adsorbates. Nevertheless, the contribution of water adsorption to Q_{net} was insignificant in comparison with that of strong organic adsorbates (e.g., PA). Table 1 also shows that the intercept values did not change much with the variation of PA concentrations ranging from 25-31 μC. This variation can be attributed to the fact that the water concentrations were relatively constant (e.g., 56M) at different PA concentrations.

Adsorption thermodynamics

In-situ adsorption measurement of PA illustrated in Fig. 5(a) also indicates that after a period of 20 min, the adsorption process has reached equilibrium for all concentrations from 2.5 μM to 25 μM. It took slightly less time to reach the adsorption equilibrium for this mixed-phase electrode than that for the anatase electrode in the *ex-situ* study (ca. 30 min), which is very likely due to the TiO_2 film thickness for the mixed-phase electrode

(i.e., 500nm) is significantly thinner than that for the anatase electrode (i.e., 1μm). Thinner thickness of the TiO_2 film apparently facilitates faster mass transport of adsorbate from film surface to the film inside.

Adsorption behaviour of organic compounds on TiO_2 surfaces commonly follows Langmuir adsorption model [8, 28, 29]. Assuming monolayer adsorption, the surface coverage, θ, can be defined as the amount ratio of occupied sites to the total adsorption sites. Because the amount of occupied sites is directly proportional to the charge, i.e., Q, θ can be expressed by the ratio of the measured net charge (Q_{net}) to the maximum net charge (Q_{max}) at 100% surface coverage [8], i.e.,

$$\theta = \frac{Q_{net}}{Q_{max}} \tag{6}$$

Because of the large ratio of solution volume (i.e., 100ml) to the electrode geometric area ($0.75cm^2$) in our adsorption study setup, there was no significant change in the bulk adsorbate concentration (C) during the adsorption and photoelectrochemical measurement processes. In other words, our setup meets another assumption of Langmuir isotherm. Assuming K is the adsorption equilibrium constant, Langmuir isotherm equation can be then written as

$$\frac{C}{Q_{net}} = \frac{1}{Q_{max}} C + \frac{1}{Q_{max}} \frac{1}{K} \tag{7}$$

The net charges Q_{net}, obtained from Fig. 5 after 20 minutes of adsorption time, and the corresponding PA concentrations are treated to fit the Langmuir model (i.e., Eqn. 7) by plotting C/Q_{net} against C to obtain a straight trendline as indicated in Fig. 7. The linear relationship ($R^2 = 0.9829$) suggests the adsorption behaviour of PA on TiO_2 electrode

surface being in good agreement with the Langmuir model, and the adsorbate molecules form a monolayer coverage on the TiO_2 surface.

According to Eqn. 7, from the gradient and the intercept of the best-fit trendline, Q_{max} and K of the mixed phase electrode are calculated to be 1.12 mC and 1.7×10^5 M^{-1}, respectively. The Q_{max} of the single phase (i.e., anatase film) by *ex-situ* method （i.e., 4.19 mC [8]）was >3 times higher than that of the mixed phase electrode. This can be explained by the fact that the anatase TiO_2 electrode (treated at 450°C) has a larger thickness (1 μm [8]) and higher porosity than the mixed phase electrode (500nm) that was treated at 700°C [23]. In comparison of the resulting K value of the mixed phase TiO_2 electrode measured by this *in-situ* method to the result of the anatase phase TiO_2 electrode from the *ex-situ* study (i.e., 4.0×10^4 M^{-1})[8], the mixed-phase K value is approximately 5 times greater than that obtained from the single-phase electrode. The greater K value of the rutile-anatase mixed phase coincides with its synergetic effect that bestows the mixed phase electrodes with an exceptional ability to mineralize organic compounds and remarkable resistance to the inhibition by aromatic compounds [23]. This is in strong contrast with the single anatase phase TiO_2 that is readily poisoned by KHP .

4. Conclusions

The adsorption amount of adsorbates on titania surface can be determined by the proposed *in-situ* photoelectrochemical technique. The proposed method can directly quantify the amount of adsorbates at titania surface in a sensitive, reproducible and accurate manner, hence provides a powerful tool for the adsorption process study. In a short period time (e.g., less than 30s) and in low adsorbate concentration range, the

adsorption reaction rate was found to be equal to the degradation rate, which provides a strong support for the proposed adsorption measurement method. This proposed method may be used to investigate the adsorption behaviour of weak adsorbates, where the weak adsorbates on the TiO_2 may be removed (partly or completely) by the post-adsorption washing process in the *ex-situ* method. Using the obtained data from the *in-situ* measurement, thermodynamic analysis indicated that the adsorption process fits the Langmuir isothermal model.

Acknowledgements:

The authors appreciate Australian Research Council for the financial support of this work.

References

[1] M.R. Hoffmann, S.T. Martin, W. Choi, D.W. Bahnemann, Chem. Rev. (Washington, D. C.) 95 (1995) 69-96.
[2] L. Tomcsányi, A. De Battisti, Electrochim. Acta 41 (1996) 2917-19.
[3] J.A. Byrne, B.R. Eggins, J. Electroanal. Chem. 457 (1998) 61-72.
[4] P.V. Kamat, Chem. Rev. (Washington, DC, United States) 93 (1993) 267-300.
[5] M. Gratzel, Nature (London, United Kingdom) 414 (2001) 338-44.
[6] K. Vinodgopal, S. Hotchandani, P.V. Kamat, J. Phys. Chem. 97 (1993) 9040-4.
[7] J.C. Yu, W. Ho, J. Lin, H. Yip, P.K. Wong, Environ. Sci. Technol. 37 (2003) 2296-301.
[8] D. Jiang, H. Zhao, S. Zhang, R. John, G.D. Will, J. Photochem. Photobiol. A 156 (2003) 201-06.
[9] X.Z. Li, H. Liu, L.F. Cheng, H.J. Tong, J. Chem.Technol. Biotechnol. 79 (2004) 774-81.
[10] Y. Xu, C.H. Langford, Langmuir 17 (2001) 897-902.
[11] C.-y. Wang, H. Groenzin, M.J. Shultz, J. Am. Chem. Soc. 127 (2005) 9736-44.
[12] C.-Y. Wang, H. Groenzin, M.J. Shultz, J J. Am. Chem. Soc. 126 (2004) 8094-95.
[13] G. Capecchi, M.G. Faga, G. Martra, S. Coluccia, M.F. Iozzi, M. Cossi, Res. Chem. Intermediat. 33 (2007) 269-84.
[14] T. Lana-Villarreal, J.M. Perez, R. Gomez, Comptes Rendus Chimie 9 (2006) 806-16.
[15] T. Tachikawa, S. Tojo, M. Fujitsuka, T. Majima, J. Phys.Chem. B 108 (2004) 5859-66.

[16] S.W. Lam, K. Chiang, T.M. Lim, R. Amal, G.K.C. Low, J. Photochem. Photobiol. A 187 (2007) 127-32.
[17] H. Hidaka, H. Honjo, S. Horikoshi, N. Serpone, Catal. Comm. 7 (2006) 331-35.
[18] T. Lana-Villarreal, A. Rodes, J.M. Perez, R. Gomez, J. Am. Chem. Soc. 127 (2005) 12601-11.
[19] N.A. Lange, J.A. Dean, Lange's handbook of chemistry, McGraw-Hill, New York ; Sydney, 1999.
[20] J. Moser, S. Punchihewa, P.P. Infelta, M. Graetzel, Langmuir 7 (1991) 3012-18.
[21] M.K. Nazeeruddin, A. Kay, I. Rodicio, R. Humphry-Baker, E. Mueller, P. Liska, N. Vlachopoulos, M. Graetzel, J. Am. Chem. Soc. 115 (1993) 6382-90.
[22] S. Zhang, D. Jiang, H. Zhao, Environ. Sci. Technol. 40 (2006) 2363-68.
[23] D. Jiang, S. Zhang, H. Zhao, Environ. Sci. Technol. 41 (2007) 303-08.
[24] A. Fujishima, T. Inoue, K. Honda, J. Am. Chem. Soc. 101 (1979) 5582-8.
[25] H. Zhao, D. Jiang, S. Zhang, K. Catterall, R. John, Anal. Chem. 76 (2004) 155-60.
[26] D. Jiang, H. Zhao, S. Zhang, R. John, J. Catal. 223 (2004) 212-20.
[27] D. Jiang, H. Zhao, S. Zhang, R. John, J. Photochem. Photobiol. A 177 (2006) 253-60.
[28] J. Cunningham, G. Al-Sayyed, J. Chem. Soc., Farad.Trans. 86 (1990) 3935-41.
[29] K.D. Dobson, P.A. Connor, A.J. McQuillan, Langmuir 13 (1997) 2614-16.

Figure Captions:

Fig. 1. LSVs at a light intensity of 6.6mW/cm^2 and a sweeping rate of 10mV/s: (a) the LSVs of the mixed-phase electrode at various PA concentrations; (b) the LSVs after the subtraction of the background LSV (0 μM PA),

Fig. 2. A typical *in-situ* transient photocurrent–time profile for various pre-adsorption time (i.e., dark time), in a solution of 5 μM PA at pH 4.0.

Fig. 3. (a) The determination of the limiting current (i_L); (b) the relationships between the limiting currents and PA concentrations at UV light intensities of 8.1, 6.6, 4.5 mW/cm^2, respectively.

Fig. 4. The determination of adsorbed organic compound using the *in-situ* adsorption measurement.

Fig. 5. The relationship between Q_{net} obtained from the *in-situ* adsorption measurement in a long time scale (a) and in a short time scale (b).

Fig. 6. The slopes (adsorption reaction rate) obtained from Table 1 was dependent on the PA concentrations.

Fig. 7. The fitting of the isotherm to Langmuir adsorption model.

Table 1. The slopes and intercepts obtained by linear regression using data from *in-situ* adsorption measurement in a short time scale (Fig. 5b).

[PA] μM	slope (μC/s)	intercept (μC)
25	6.9474	30.358
20	5.864	30.943
15	4.5163	25.64
10	3.3583	26.112
5	1.9325	29.851
2.5	1.4053	25.879

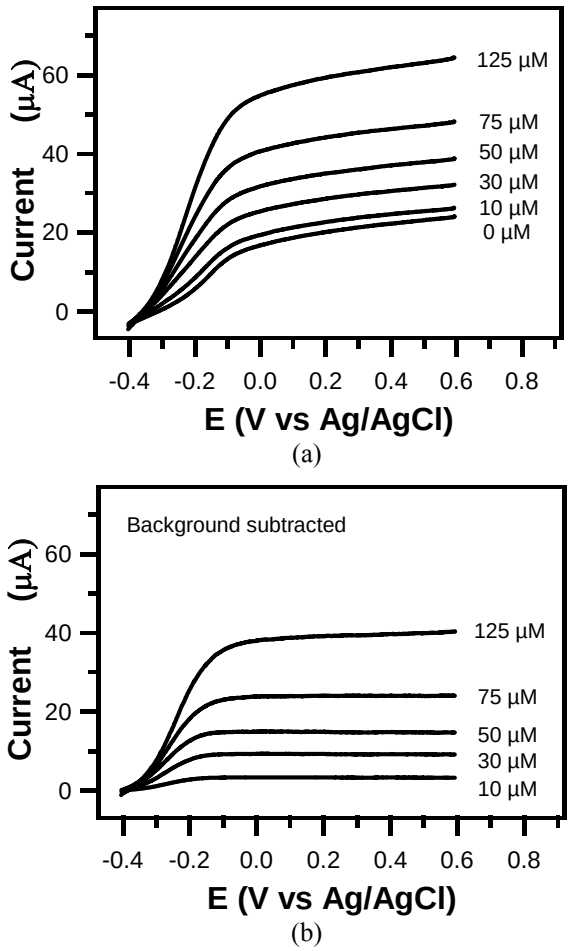
Current (μA)
60
40
20
0
125 μM
75 μM
50 μM
30 μM
10 μM
0 μM
-0.4 -0.2 0.0 0.2 0.4 0.6 0.8
E (V vs Ag/AgCl)
(a)
Background subtracted
Current (μA)
60
40
20
0
125 μM
75 μM
50 μM
30 μM
10 μM
-0.4 -0.2 0.0 0.2 0.4 0.6 0.8
E (V vs Ag/AgCl)
(b)

Fig. 1

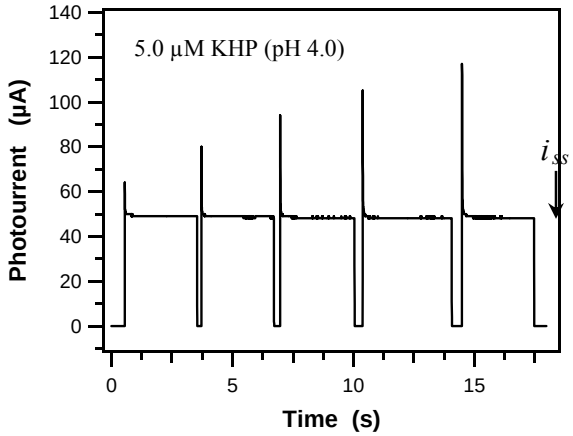
5.0 µM KHP (pH 4.0)
Photourrent (µA)
Time (s)
i_{ss}
0
20
40
60
80
100
120
140
0
5
10
15

Fig. 2

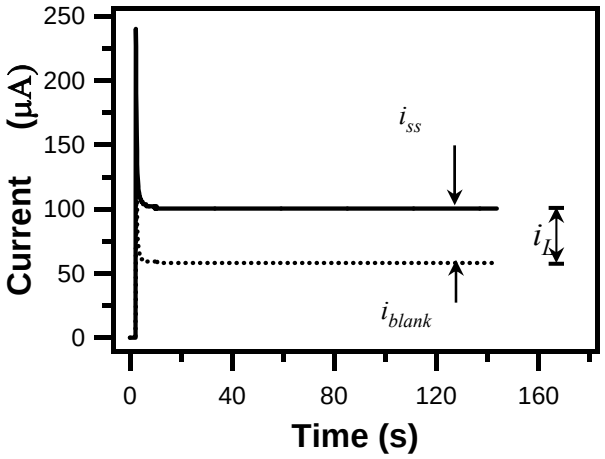
250
200
150
100
50
0
Current (μA)
i_{ss}
i_L
i_{blank}
0
40
80
120
160
Time (s)

(a)

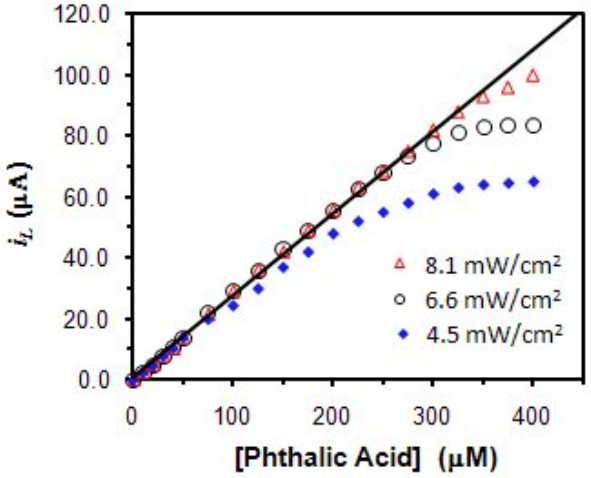
120.0
100.0
80.0
60.0
40.0
20.0
0.0
i_L (μA)
8.1 mW/cm²
6.6 mW/cm²
4.5 mW/cm²
0
100
200
300
400
[Phthalic Acid] (μM)

(b)

Fig. 3

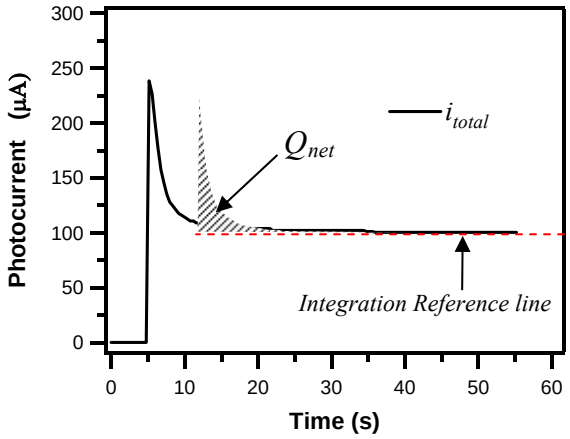
Photocurrent (μA)
300
250
200
150
100
50
0
0
10
20
30
40
50
60
Time (s)
i_{total}
Q_{net}
Integration Reference line

Fig. 4

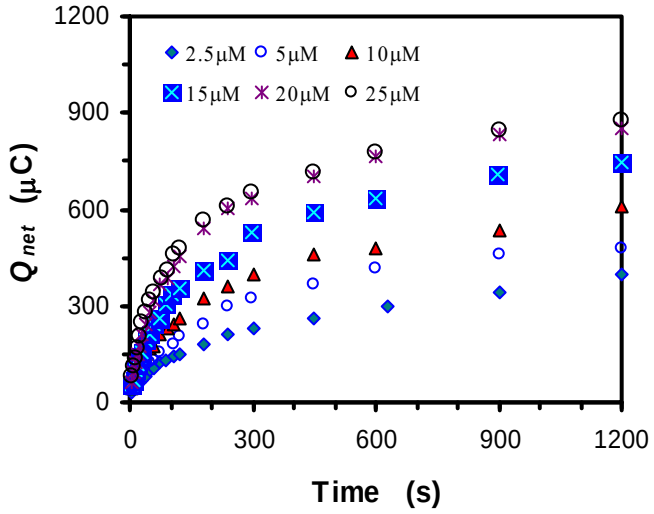
2.5μM
5μM
10μM
15μM
20μM
25μM
Q_{net} (μC)
Time (s)
0
300
600
900
1200

(a)

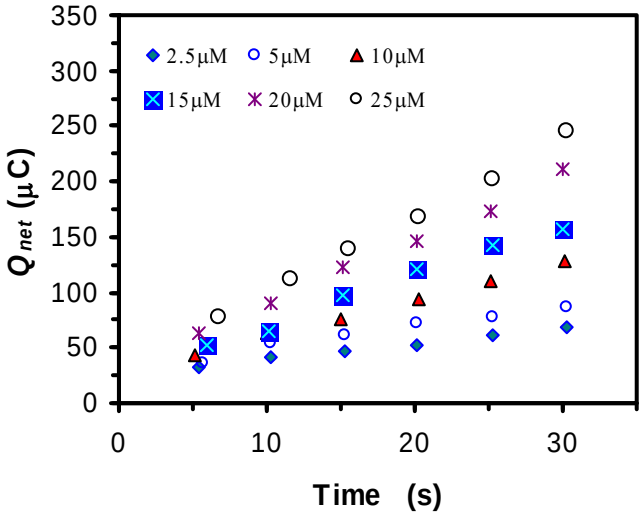
2.5μM
5μM
10μM
15μM
20μM
25μM
Q_{net} (μC)
Time (s)
0
50
100
150
200
250
300
350
10
20
30

(b)

Fig. 5

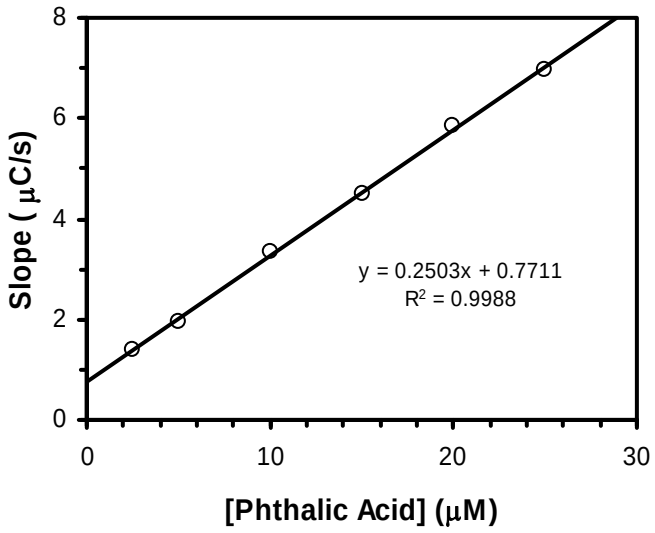
Slope (µC/s)
[Phthalic Acid] (µM)
y = 0.2503x + 0.7711
R² = 0.9988
0
2
4
6
8
0
10
20
30

Fig. 6

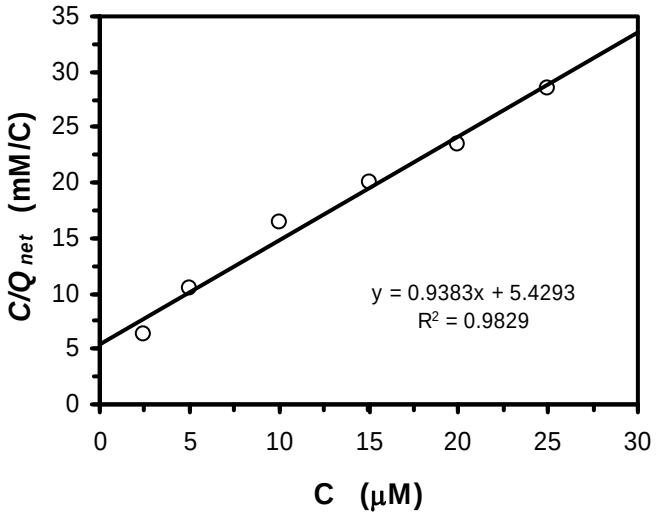
35
30
25
20
15
10
5
0
0
5
10
15
20
25
30
C/Q net (mM/C)
C (μM)
y = 0.9383x + 5.4293
R2 = 0.9829

Fig. 7.